

# StableMoFusion: Towards Robust and Efficient Diffusion-based Motion Generation Framework

Yiheng Huang  
Beijing University of Posts  
and Telecommunications  
hyh654@bupt.edu.cn

Hui Yang  
CAIR, HKISI, Chinese  
Academy of Sciences<sup>1</sup>

Chuanchen Luo  
Institute of Automation,  
Chinese Academy of  
Sciences

Yuxi Wang  
CAIR, HKISI, Chinese  
Academy of Sciences<sup>1</sup>

Shibiao Xu  
Beijing University of Posts  
and Telecommunications

Zhaoxiang Zhang  
Institute of Automation,  
Chinese Academy of  
Sciences

Man Zhang\*  
Beijing University of Posts  
and Telecommunications  
zhangman@bupt.edu.cn

Junran Peng<sup>†</sup>  
University of Science and  
Technology Beijing  
jrpeng4ever@126.com

## Abstract

Thanks to the powerful generative capacity of diffusion models, recent years have witnessed rapid progress in human motion generation. Existing diffusion-based methods employ disparate network architectures and training strategies. The effect of the design of each component is still unclear. In addition, the iterative denoising process consumes considerable computational overhead, which is prohibitive for real-time scenarios such as virtual characters and humanoid robots. For this reason, we first conduct a comprehensive investigation into network architectures, training strategies, and inference process. Based on the profound analysis, we tailor each component for efficient high-quality human motion generation. Despite the promising performance, the tailored model still suffers from foot skating which is an ubiquitous issue in diffusion-based solutions. To eliminate footskate, we identify foot-ground contact and correct foot motions along the denoising process. By organically combining these well-designed components together, we present StableMoFusion, a robust and efficient framework for human motion generation. Extensive experimental results show that our StableMoFusion performs favorably against current state-of-the-art methods. Project page: <https://h-y1heng.github.io/StableMoFusion-page/>.

## 1 Introduction

Human motion generation aims to generate natural, realistic, and diverse human motions, which could be used for animating virtual characters or manipulating embodied robots to imitate vivid and rich human movements without long-time manual motion modeling and professional skills [3, 28]. It shows great potential in the fields of animation, video games, film production, human-robot interaction, and *etc.* Recently, the application of diffusion models to human motion generation has led to significant improvements in the quality of generated motions [2, 20, 28].

Despite the notable progress made by diffusion-based motion generation methods, its development is still hindered by several fragmented and underexplored issues: 1) **Lack of Systematic Analysis**: these diffusion-based motion generation work usually employ

\*Corresponding author

<sup>†</sup>Project Leader

<sup>1</sup> Centre for Artificial Intelligence and Robotics, Hong Kong Institute of Science & Innovation.

**Table 1: StableMoFusion achieves superior performance. Lower FID and higher R Precision mean, the better.**

Method	FID↓	R Precision (top3)↑
MDM [20]	0.544	0.611
MLD [2]	0.473	0.772
MotionDiffuse [28]	0.630	0.782
ReMoDiffuse [29]	0.103	0.795
StableMoFusion (Ours)	<b>0.098</b>	<b>0.841</b>

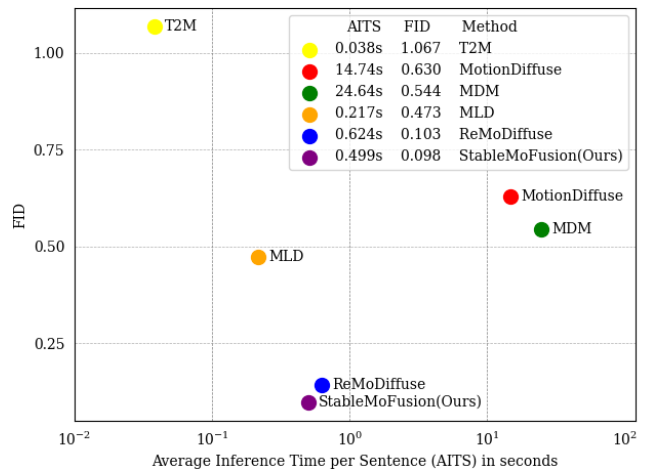


**Figure 1: Comparison of the inference time costs on motion generation. The closer the model is to the origin, the better.**

different network architectures and training pipelines, which hinders cross-method integration and the adoption of advancements from related domains. 2) **Long Inference Time**: due to the time-consuming iterative sampling process, most existing methods are impractical for applications with virtual characters and humanoid robots, where real-time responsiveness is crucial. 3) **Footskate Issue**: foot skating in generated motions remains a major concern. This significantly undermines the quality of generated motions and limits their practical applicability.

Therefore, in order to fill these research gaps and enhance the effectiveness and reliability of diffusion-based motion generation

in practical applications, our study conducts a comprehensive and systematic investigation through network architectures, training strategies, and inference process, to reveal the influence of each factor. Ultimately, based on our observations, we present a robust and efficient framework for diffusion-based motion generation, called **StableMoFusion**, as illustrated in Figure 2.

In StableMoFusion, we use Conv1D UNet with AdaGN and linear cross-attention as the motion-denoising network and improve its generalization capability with GroupNorm tweak. During training, two effective strategies were employed to enhance the network’s ability to generate motion. During inference, we use four training-free acceleration tricks to achieve efficient inference. Furthermore, we present a footskate cleanup method based on a mechanical model and optimization.

Extensive experiments demonstrate that StableMoFusion achieves an excellent trade-off between text-motion consistency and motion quality compared to other state-of-the-art methods, as shown in Table 1. Meanwhile, StableMoFusion’s efficient inference process notably reduces the number of iterations required for generation from 1000 to 10, as well as shorter inference times than methods of about the same performance, achieving an average inference time of 0.5 seconds on the Humanm3D test set, as shown in Figure 1. In addition, our footskate cleanup method within diffusion framework sizably solves the foot skating problem of motion generation as shown in Section 5.4.

Our major contributions can be summarized as follows:

- We perform a systematic evaluation and analysis on the design of each component in the diffusion-based motion generation pipeline, including network architectures, training strategies, and inference process.
- We propose an effective mechanism to eliminate foot skating which is a comment issue in current methods.
- By consolidating these well-designed components, we present a robust and efficient diffusion-based motion generation framework named *StableMoFusion*. Extensive experiments demonstrate its superiority in text-motion consistency and motion quality.

## 2 Related Work

### 2.1 Motion Diffusion Generation

Recent advancements in diffusion models have greatly enhanced human motion generation quality. Notable works include Motion-Diffuse [28], which integrates text features via cross-attention; MDM [20], exploring various denoising networks with Transformer or GRU; PhysDiff [26], adding realism with physical constraints; MLD [2], accelerating generation using VAE latent spaces; and Re-MoDiffuse [29], enhancing with retrieval mechanisms. MotionLCM [4] achieves real-time controllable motion generation through latent consistency model.

However, the field of motion generation is still grappling with a lack of consistent and fair comparisons due to varying network architectures, sampling methods, training strategies, etc. Our work addresses this by providing a thorough exploration of these aspects, revealing the influence of each factor.

### 2.2 Footskate Cleanup

In order to generate realistic motions in computer animation, various methods have been developed to improve footskate issue.

Edge [21] embeds the foot contact term into the action representation for training and applies Contact Consistency Loss as a constraint to keep the physical plausibility of motion. RFC [25], Drop [10] and Physdiff [26] use reinforcement learning to constrain the physical states of actions, such as ground force reaction and collision situations to get a realism motion. UnderPressure [14] and GroundLink [7] respectively collect foot force datasets during motion. UnderPressure [14] also utilizes this dataset to train a network capable of predicting vertical ground reaction forces.

Based on this, Our approach uses a novel module to optimize the sliding of the weighted feet in diffusion-generated motions during inference by backpropagation. Compared to traditional feet-joint loss during training, our offline-extendable and force-based method is more stable and reliable for the animation industry.

## 3 Preliminaries

The pipeline of Diffusion model [8] involves three processes: a **forward process** that gradually diffuses noise into the sample, a **reverse process** that optimizes a network to eliminate the above perturbation from noisy samples, and an **inference process** that utilizes the trained network to iteratively denoise noisy samples.

Specifically,  $x_0 \in R^{N \times M}$  represents a sequence of human poses for N frames, where M is the dimension of human pose representations. Then randomly select a timestep  $t \sim U[0, T]$  and the noisy motion  $x_t$  after t-step diffusion is gained by Equation 1,

$$x_t = \sqrt{\alpha_t}x_0 + \sqrt{1 - \alpha_t}\epsilon \quad (1)$$

where  $\epsilon$  is a Gaussian noise.  $\sqrt{\alpha_t}$  and  $\sqrt{1 - \alpha_t}$  are the strengths of signal and noise, respectively.  $\alpha_t$  decreases as t increases. When  $\sqrt{\alpha_t}$  is small enough, we can approximate  $x_t \sim \mathcal{N}(0, I)$ .

Next, given a motion-denoising model  $G_\theta(x_t, t, c)$  for predicting the original sample, parameterized by  $\theta$ , the optimization can be formulated as follows:

$$\min_{\theta} E_{t \sim U[0, T], x_0 \sim p_{data}} \|G_\theta(x_t, t, c) - x_0\|_2^2 \quad (2)$$

In the inference process, a trained motion-denoising network can progressively generate samples from noise with various samplers. For instance, DDPM [8] iteratively denoise the noisy data from  $t$  to a previous timestep  $t'$ , as shown in Algorithm 1.

---

#### Algorithm 1 Inference

---

```

Given a text prompt  $c$ 
 $x_t \sim \mathcal{N}(0, I)$ 
for  $t = T$  to 1 do
   $\tilde{x}_0 = G(x_t, t, c)$ 
   $\epsilon \sim \mathcal{N}(0, I)$  if  $t > 1$ , else  $\epsilon = 0$ 
   $x_{t-1} = \frac{\sqrt{\alpha_{t-1}}\beta_t}{1-\alpha_t}\tilde{x}_0 + \frac{\sqrt{\alpha_t}(1-\alpha_{t-1})}{1-\alpha_t}x_t + \tilde{\beta}_t\epsilon$ 
end for
return  $x_0$ 

```

---

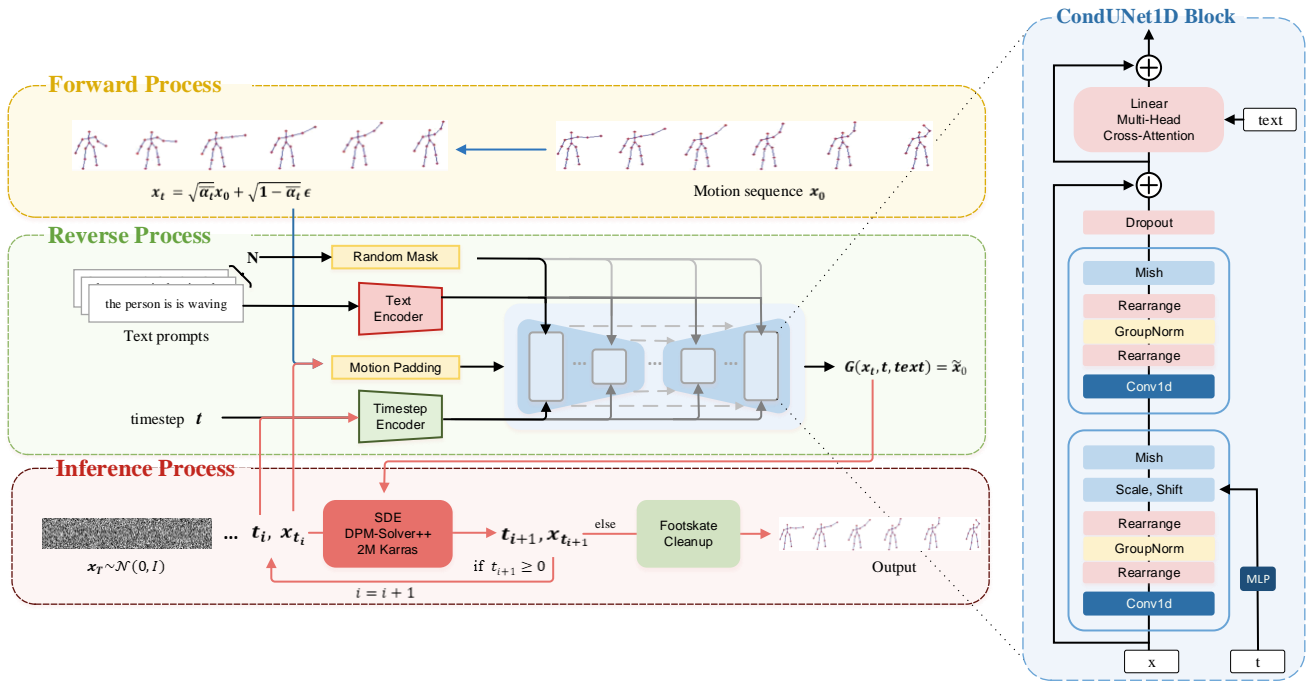


Figure 2: Overview of StableMoFusion, which is composed of a diffusion forward process, a reverse process on CondUNet1D motion-denoising network, and an efficient inference. The colors of the arrows indicate different stages: blue for training, red for inference, and black for both.

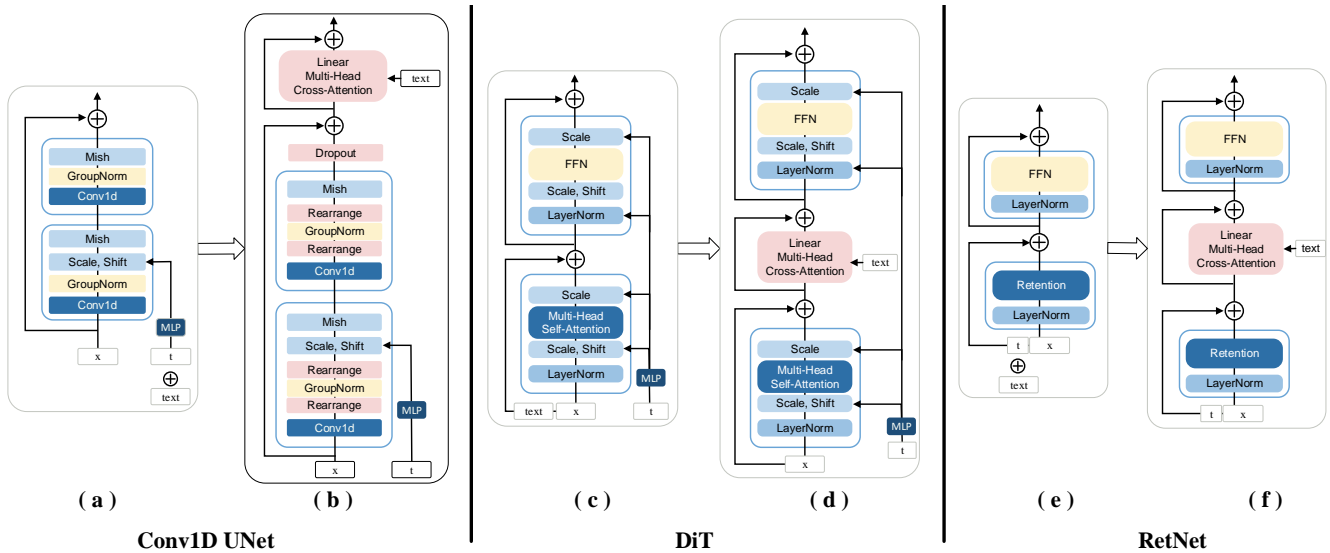


Figure 3: Visualization of the block structure and their adjustments of Conv1D UNet, DiT and RetNet. Pink blocks indicate structures that have been added or modified.

## 4 Method

Through comprehensive exploratory experiments conducted on diffusion-based motion generation, we propose a novel diffusion framework, named StableMoFusion, as illustrated in Figure 2, to

facilitate robust and efficient motion generation. This section begins with our investigation of the architecture of motion-denoising networks. Next, we discuss several training strategies pivotal for enhancing model performance in Section 4.2. Subsequently, we introduce our improvements in the inference process in Section 4.3,

tailored to enable efficient inference. Lastly, we discuss and present a solution to the footskate issue in Section 4.4.

## 4.1 Model Architecture

In this subsection, we explore three motion denoising network architectures for text-to-motion generation tasks: Conv1D UNet [3, 11], Diffusion Transformer (DiT) [15] and the latest Retentive Network (RetNet) [19].

### 4.1.1 Conv1D UNet.

*Baseline.* We choose the Conv1D UNet with AdaGN [5] as the baseline, where each block is shown as Figure 3 (a). The skip connections and layer-by-layer reconstruction mechanism of UNet, as shown in Figure 2, are well-suited for retaining spatial and temporal details in motion sequences. Moreover, UNet can extract and reconstruct features at different scales, producing more realistic motion sequences.

In the Conv1d block, the Clip-based [17] sentence-level textural embedding,  $c_{text} \in R^D$ ,  $D$  is the dimension of text, is projected into *scale* and *shift* along with timestep embedding for feature-wise linear modulation (FiLM):  $x^{(i)} \times (1 + scale) + shift$ ,  $x^{(i)}$  is the  $i$ th-frame pose embedding. That means a consistent condition-based linear mapping is applied to the pose embedding of each frame. This method is well-suited for injecting timestep into noisy motion for denoising, but falls short. This is because the entire motion sequence is subjected to the same timestep-level noise perturbation, while each frame of the motion sequence involves distinct semantics within the text sentence.

*Block Adjustment.* We integrated Residual Cross-Attention into the Conv1D block for alignment of motion embeddings (as Query) with word-level semantics (as Key and Value). In addition, dropout is added to boost model generalization, as depicted in Figure 3 (b). Beyond the baseline’s sentence-level embedding, we employ additional transformer layers that follow CLIP to refine word-level text embeddings into motion-related representations,  $c_{text} \in R^{L \times D}$ ,  $L$  is the length of text, for effective cross-modality attention.

*GroupNorm Tweak.* We rearranged the dimensions of motion embedding to enable feature-wise Group Normalization, as depicted in Figure 3 (b). Given that Conv1D performs convolutions along the sequence dimension, directly applying group normalization to its output is akin to sequence-wise normalization, which is highly sensitive to the proportion of sequence padding. Consequently, the baseline model experiences a significant performance drop on datasets with diverse motion lengths, such as KIT-ML, due to the increased impact of padding.

### 4.1.2 Diffusion Transformer.

*Baseline.* To explore the effectiveness of the DiT structure for motion generation, we replace the Vision Transformer used for images in the DiT with self-attention used for motion data as the baseline, with the basic block structure shown in Figure 3 (c). For text-to-motion generation, we embed text prompts via the CLIP [17] encoder and project them into tokens concatenated with motion embeddings for self-attention. It scales and shifts the motion embedding before and after each autoregressive computation using

timestep, which ensures the motion-denoising trajectory is closely aligned with the timestep.

*Block Adjustment.* We have also tried to incorporate Linear Multi-Head Cross-Attention into the DiT framework, as shown in Figure 3 (d). This adjustment allows for a more nuanced fusion of textual cues with motion dynamics than fusing all the text information into the one-dimensional text embedding in baseline, which enhances the coherence and relevance of generated motion sequences.

### 4.1.3 Retentive Network.

*Baseline.* Our RetNet baseline follows a straightforward implementation similar to MDM, where the timesteps encoding is concatenated with the textual projection to form tokens, which are then fed along with motion embeddings into RetNet, with its basic block shown in Figure 3 (e). RetNet incorporates a gated multi-scale retention mechanism, which enhances information retention and processing capabilities, thereby enabling nuanced comprehension and generation of motion sequences. Through our investigation, we aim to ascertain the feasibility of leveraging RetNet for motion generation tasks.

*Block Adjustment.* To further integrate textual information, we also employ Linear Multi-Head Cross-Attention between retention and FFN, as shown in Figure 3 (f). By segregating temporal and textual features, our approach aims to preserve the distinct characteristics of each modality and allow the model to independently learn and leverage relevant cues for motion generation. This separation enhances the model’s interpretability and flexibility, enabling it to better capture the intricacies of both temporal dynamics and semantic context.

### 4.1.4 Final Model Architecture.

Ultimately, we choose the Conv1D UNet with block adjustment and GroupNorm tweak as the motion-denoising model of StableMoFusion, as shown in Figure 2. We call this network as CondUNet1D. Both DiT and RetNet use the idea of attention to activate the global receptive field in the temporal dimension, which benefits the modeling of long-range dependency. The receptive field of Conv1D UNet is mainly in the convolution kernel window, promoting a coherent and smooth transition between frames. We tend to prioritize smoother generation in current applications of motion generation.

In our StableMoFusion, we set the base channel and channel multipliers of UNet to 512 and [2,2,2,2] respectively. For text encoder, we leverage pre-trained CLIP [17] token embeddings, augmenting them with four additional transformer encoder layers, the same as MotionDiffuse [28], with a latent text dimension of 256. For timesteps encoder, it is implemented using position encoding and two linear layers, the same as StableDiffusion [18], with a latent time dimension of 512.

## 4.2 Training Strategies

Recent research has shown that training strategies in diffusion models are also crucial for generation capabilities [1]. In this subsection, we will analyze the impact of two empirically valid training strategies on diffusion-based motion generation: exponential moving average and classifier-free guidance.

#### 4.2.1 Exponential Moving Average.

Exponential Moving Average (EMA) calculates a weighted average of a series of model weights, giving more weight to recent data. Specifically, assume the weight of the model at time  $t$  as  $\theta_t$ , then the EMA formulated as:  $v_t = \beta \cdot v_{t-1} + (1 - \beta) \cdot \theta_t$ , where  $v_t$  denotes the average of the network parameters for the first  $t$  iterations ( $v_0 = 0$ ), and  $\beta$  is the weighted weight value.

During the training of the motion-denoising network, the network parameters change with each iteration, and the motion modeling oscillates between text-motion consistency and motion quality. Therefore, the use of EMA can smooth out the change process of these parameters, reduce mutations and oscillations, and help to improve the stability ability of the motion-denoising model.

#### 4.2.2 Classifier-Free Guidance.

To further improve the generation quality, we use Classifier-Free Guidance (CFG) to train the motion-denoising generative model. By training the model to learn both conditioned and unconditioned distributions (e.g., setting  $c = \emptyset$  for 10% of the samples), CFG ensures that the models can effectively capture the underlying data distribution across various conditions. In inference, we can trade-off text-motion consistency and fidelity using  $s$ :

$$G_s(x_t, t, c) = G(x_t, t, \emptyset) + s \cdot (G(x_t, t, c) - G(x_t, t, \emptyset)) \quad (3)$$

This ability to balance text-motion consistency and fidelity is crucial for producing varied yet realistic outputs, enhancing the overall quality of generated motion.

### 4.3 Efficient Inference

Time-consuming inference time remains a major challenge for diffusion-based approaches. To address this problem, we improve inference speed by integrating four efficient and training-free tricks in the inference process: 1) efficient sampler, 2) embedded-text cache, 3) parallel CFG computation, and 4) low-precision inference.

#### 4.3.1 Efficient Sampler.

We replace DDPM with a more efficient sampling algorithm, DPM-Solver++ [13], to reduce denoising iterations during inference. Specifically, we utilize the SDE variant of second-order DPM-Solver, a high-order solver for diffusion stochastic differential equations (SDEs). It introduces additional noise during the iterative sampling. Thereby, the stochasticity of its sampling trajectories helps to reduce the cumulative error [24], which is crucial for the realism of generated motion. In addition, we adopt the Karras Sigma [?] to set discrete timesteps. This method leverages the theory of constant-velocity thermal diffusion to determine optimal timesteps, thereby maximizing the efficiency of motion denoising within a given number of iterations.

#### 4.3.2 Embedded-text Cache.

We integrate the Embedded-text Cache mechanism into the inference process to avoid redundant calculations. In diffusion-based motion generation, the text prompts remain unchanged across iterations, resulting in the same embedded text in each computation of the denoising network. Specifically, we compute the text embedding initially and subsequently utilize the embedded text directly in each network forward, thereby reducing computational redundancy and speeding up inference.

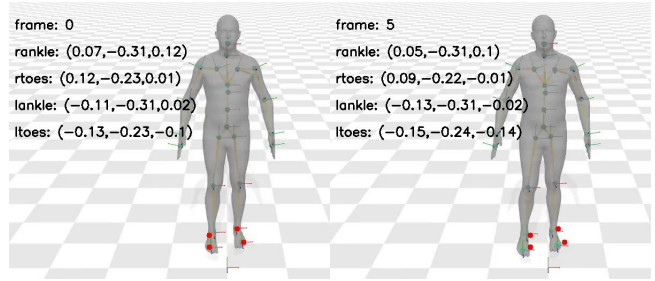


Figure 4: Footskate for a 20fps motion, with positional offsets of both feet from frame 0 (red) to frame 5 (green).

#### 4.3.3 Parallel CFG Computation.

We implement the inference process of CFG in parallel to speed up the single iteration calculation while maintaining model generation performance. Due to the CFG mechanism Equation 3, in each iterative step during inference, it is necessary to execute conditional and unconditional denoising, respectively, using the trained motion network, and then sum up the results.

#### 4.3.4 Low-precision Inference.

We utilize half-precision floating point (FP16) computation during inference to accelerate processing. Newer hardware supports enhanced arithmetic logic units for lower-precision data types. By applying parameter quantization, we convert FP32 computations to lower-precision formats, effectively reducing computational demands, parameter size, and memory usage of the model.

### 4.4 Footskate Reduction

Foot skating is an animation artifact where a character’s feet move unrealistically, often sliding across the ground, despite the character’s body remaining in a consistent pose. Figure 4 illustrates an instance of the foot skating phenomenon. The depicted frames, separated by a 0.25-second interval, show the same posture but with both feet having shifted positions. Ideally, for this motion, we aim for the feet to maintain a consistent anchor point. Commonly, selecting the foot position from the midpoint of a foot skating sequence as fixed helps to minimize disruptions to surrounding frames.

The key to eliminating foot skating is to first identify the foot joints and frame ranges where foot skating occurs, and then anchor those keypoints at their positions  $p$  in the intermediate frames. We formulate this constraint as a loss term shown in Equation 4 where  $j$  indicates joint and  $f$  is frame ranges.

$$L_{foot} = \sum_j^{J_{skating}} \sum_f^{F_{skating}} (P_j - p) \quad (4)$$

$J_{skating}$  contains all the joints where foot skating may occur, specifically including the right ankle, right toes, left ankle, and left toes.  $F_{skating}$  is a collection of all frame ranges of the joint  $j$ .  $P_j$  means the positions of joint  $j$ . We incorporate Equation 4 to a gradient descent algorithm to correct foot skating motion.

Following UnderPressure [14], we use vertical ground reaction forces (vGRFs) to identify foot joint  $j$  and its skating frames  $f$ . The

vGRFs prediction model of UnderPressure  $V_{23}$  requires motion of a predefined 23 joints skeleton  $S_{23}$ , which is different from our motion data. In our work, we utilize HumanML3D [6] with 22 skeletal joints  $S_{22}$  and KIT-ML [16] motion with 21 skeletal joints. The subsequent foot skating cleanup primarily focused on HumanML3D. We transferred the pre-trained weights of  $V_{23}$  to our own model  $V_{22}^\theta$  using the constraints Equation 5, enabling us to directly predict the vertical ground reaction forces for HumanML3D motions.  $P$  is keypoints of HumanML3D motion.  $P_{S_{23}}$  is the result of retargeting  $P$  to skeleton  $S_{23}$ .

$$\min_{\theta} \|V_{22}^\theta(P) - V_{23}(P_{S_{23}})\|_2^2 \quad (5)$$

$$L = \omega_q L_{\text{pose}} + \omega_f L_{\text{foot}} + \omega_t L_{\text{trajectory}} + \omega_v L_{\text{vGRFs}} \quad (6)$$

$$L_{\text{foot}} = L_{\text{foot}}(P, \hat{P}, V_{23}, P_{S_{23}}) \quad (7)$$

$$L_{\text{vGRFs}} = L_{\text{vGRFs}}(P, \hat{P}, V_{22}^\theta) \quad (8)$$

Drawing inspiration from UnderPressure [14], we use foot contact loss  $L_{\text{foot}}$  to fix contact joints, pose loss  $L_{\text{pose}}$  and trajectory loss  $L_{\text{trajectory}}$  to keep the semantic integrity of motion, vGRFs loss  $L_{\text{vGRFs}}$  to keep valid foot pose. Our supplementary material provides detailed definitions of these loss terms. The final definition of our loss function is as Equation 6 [14] where  $\omega_q, \omega_f, \omega_t, \omega_v$  are weights of its loss item.  $P$  is keypoints of footskating motion and  $\hat{P}$  is the result keypoints after footskate cleanup.

Through our method, the footskate cleanup process can be generalized to various skeletal motions.

In a few cases, motion corrected by Equation 6 may occur unreasonable or unrealistic poses. The diffusion model trained on a large amount of motion data learns the prior knowledge of real motions and has the ability to correct the invalid motions.

Therefore, we use our pretrained diffusion model to correct such cases. Motivated by OmniControl [23] and Physdiff [26], we incorporate footskate cleaning method into the diffusion denoising process, denoted as StableMoFusion\*.

## 5 Experiments

### 5.1 Dataset and Evaluation Metrics

We use HumanML3D [6] and KIT-ML [16] datasets for our experiments. HumanML3D Dataset contains 14,646 motions and 44,970 motion annotations. KIT Motion Language Dataset contains 3,911 motions and 6,363 natural language annotations.

The evaluation metrics can be summarized into four key aspects: 1) Motion Realism: Fréchet Inception Distance (FID), which evaluates the similarity between generated and ground truth motion sequences using feature vectors extracted by a pre-trained motion encoder [6]. 2) Text match: R Precision calculates the average top-k accuracy of matching generated motions with textual descriptions using a pre-trained contrastive model [6]. 3) Generation diversity: Diversity measures the average joint differences across generated sequences from all test texts. Multi-modality quantifies the diversity within motions generated for the same text. 4) Time costs: Average Inference Time per Sentence (AITS) [2] measures the inference efficiency of diffusion models in seconds, considering generation batch size as 1, without accounting for model or data loading time.

In all of our experiments, FID and R Precision are the principal metrics we used to conduct our analysis and draw conclusions.

### 5.2 Implements Details

For training, we use DDPM [8] with  $T = 1,000$  denoising steps and variances  $\beta_t$  linearly from 0.0001 to 0.02 in the forward process. And we use AdamW with an initial learning rate of 0.0002 and a 0.01 weight decay to train the sample-prediction model for 50,000 iterations at batch size 64 on an RTX A100. Meanwhile, the learning rate was reduced by 0.9 per 5,000 steps. On gradient descent, clip the gradient norm to 1. For CFG, setting  $c = \emptyset$  for 10% of the samples.

For inference, we use the SDE variant of second-order DPM-Solver++ [13] with Karras Sigmas [?] in inference for sampling 10 steps. The scale for CFG is set to 2.5.

### 5.3 Quantitative Results

We compare our StableMoFusion with several state-of-the-art models on the HumanML3D [6] and KIT-ML [16] datasets in Table 2 and Table 3, respectively. Most results are borrowed from their own paper and we run the evaluation 20 times and  $\pm$  indicates the 95% confidence interval.

Our method achieves the state-of-the-art results in FID and R Precision (top k) on the HumanML3D dataset, and also achieves good results on the KIT-ML dataset: the best R Precision (top k) and the second best FID. This demonstrates the ability of StableMoFusion to generate high-quality motions that align with the text prompts. On the other hand, while some methods excel in diversity and multi-modality, it’s crucial to anchor these aspects with accuracy (R-precision) and precision (FID) to strengthen their persuasiveness. Otherwise, diversity or multimodality becomes meaningless if the generated motion is bad. Therefore, our StableMoFusion achieves advanced experimental results on two datasets and shows robustness in terms of model performance.

StableMoFusion\* focuses on the real effect of footskate cleanup. Therefore, the timestep to begin cleaning footskate during inference depends on the motion and thus the StableMoFusion\* doesn’t apply to the evaluation process of [6].

### 5.4 Qualitative Result

Figure 5 shows the qualitative results of our footskate cleanup method, StableMoFusion\*. The red bounding box of the footskate motion clearly has multiple foot outlines, whereas ours shows only one. The comparison graph shows the effectiveness of our method for cleaning footskate. Directly applying the footskate cleanup method of UnderPressure [14] to our motion would result in motion distortion, while our method effectively avoids such deformation. In our supplementary material, we will further present a comparison between our method and the UnderPressure method by videos to illustrate it.

### 5.5 Inference Time

We calculate AITS of StableMoFusion and ReMoDiffuse [29] with the test set of HumanML3D [6] on Tesla V100 as MLD [2] does, the other results of Figure 1 are borrowed from [2]. For instance, MDM [20] with CFG requires 24.74s for average inference; MotionDiffuse [28] without CFG uses condition encoding cache and still

Table 2: Quantitative results on the HumanML3D test set. The right arrow  $\rightarrow$  means the closer to real motion the better. Red and Blue indicate the best and the second best result.

Method	FID $\downarrow$	R Precision $\uparrow$			Diversity $\rightarrow$	Multi-modality $\uparrow$
		top1	top2	top3		
Real	0.002 $\pm$ .000	0.511 $\pm$ .003	0.703 $\pm$ .003	0.797 $\pm$ .002	9.503 $\pm$ .065	-
T2M [6]	1.067 $\pm$ .002	0.457 $\pm$ .002	0.639 $\pm$ .003	0.743 $\pm$ .003	9.188 $\pm$ .002	2.090 $\pm$ .083
MDM [20]	0.544 $\pm$ .044	0.320 $\pm$ .005	0.498 $\pm$ .004	0.611 $\pm$ .007	9.599 $\pm$ .086	2.799 $\pm$ .072
MLD [2]	0.473 $\pm$ .013	0.481 $\pm$ .003	0.673 $\pm$ .003	0.772 $\pm$ .002	9.724 $\pm$ .082	2.413 $\pm$ .079
MotionDiffuse [28]	0.630 $\pm$ .001	0.491 $\pm$ .001	0.681 $\pm$ .001	0.782 $\pm$ .001	9.410 $\pm$ .049	1.553 $\pm$ .042
GMD [11]	0.212	-	-	0.670	9.440	-
T2M-GPT [27]	0.116 $\pm$ .004	0.491 $\pm$ .003	0.680 $\pm$ .003	0.775 $\pm$ .002	9.761 $\pm$ .081	1.856 $\pm$ .011
MotionGPT [9]	0.232 $\pm$ .008	0.492 $\pm$ .003	0.681 $\pm$ .003	0.778 $\pm$ .002	9.528 $\pm$ .071	2.008 $\pm$ .084
ReMoDiffuse [29]	0.103 $\pm$ .004	0.510 $\pm$ .005	0.698 $\pm$ .006	0.795 $\pm$ .004	9.018 $\pm$ .075	1.795 $\pm$ .043
M2DM [12]	0.352 $\pm$ .005	0.497 $\pm$ .003	0.682 $\pm$ .002	0.763 $\pm$ .003	9.926 $\pm$ .073	3.587 $\pm$ .072
Fg-T2M [22]	0.243 $\pm$ .019	0.492 $\pm$ .002	0.683 $\pm$ .003	0.783 $\pm$ .002	9.278 $\pm$ .072	1.614 $\pm$ .049
StableMoFusion (Ours)	0.098 $\pm$ .003	0.553 $\pm$ .003	0.748 $\pm$ .002	0.841 $\pm$ .002	9.748 $\pm$ .092	1.774 $\pm$ .051

Table 3: Quantitative results on the KIT-ML test set. The right arrow  $\rightarrow$  means the closer to real motion the better. Red and Blue indicate the best and the second best result.

Method	FID $\downarrow$	R Precision $\uparrow$			Diversity $\rightarrow$	Multi-modality $\uparrow$
		top1	top2	top3		
Real Motion	0.031 $\pm$ .004	0.424 $\pm$ .005	0.649 $\pm$ .006	0.779 $\pm$ .006	11.08 $\pm$ .097	-
T2M [6]	2.770 $\pm$ .109	0.370 $\pm$ .005	0.569 $\pm$ .007	0.693 $\pm$ .007	10.91 $\pm$ .119	1.482 $\pm$ .065
MDM [20]	0.497 $\pm$ .021	0.164 $\pm$ .004	0.291 $\pm$ .004	0.396 $\pm$ .004	10.847 $\pm$ .109	1.907 $\pm$ .214
MLD [2]	0.404 $\pm$ .027	0.390 $\pm$ .008	0.609 $\pm$ .008	3.204 $\pm$ .027	10.80 $\pm$ .117	2.192 $\pm$ .071
MotionDiffuse [28]	1.954 $\pm$ .062	0.417 $\pm$ .004	0.621 $\pm$ .004	0.739 $\pm$ .004	11.10 $\pm$ .143	0.730 $\pm$ .013
T2M-GPT [27]	0.514 $\pm$ .029	0.416 $\pm$ .006	0.627 $\pm$ .006	0.745 $\pm$ .006	10.921 $\pm$ .108	1.570 $\pm$ .039
MotionGPT [9]	0.510 $\pm$ .016	0.366 $\pm$ .005	0.558 $\pm$ .004	0.680 $\pm$ .005	10.35 $\pm$ .084	2.328 $\pm$ .117
ReMoDiffuse [29]	0.155 $\pm$ .006	0.427 $\pm$ .014	0.641 $\pm$ .004	0.765 $\pm$ .055	10.80 $\pm$ .105	1.239 $\pm$ .028
M2DM [12]	0.515 $\pm$ .029	0.416 $\pm$ .004	0.628 $\pm$ .004	0.743 $\pm$ .004	11.417 $\pm$ .97	3.325 $\pm$ .37
Fg-T2M [22]	0.571 $\pm$ .047	0.418 $\pm$ .005	0.626 $\pm$ .004	0.745 $\pm$ .004	10.93 $\pm$ .083	1.019 $\pm$ .029
StableMoFusion (Ours)	0.258 $\pm$ .029	0.445 $\pm$ .006	0.660 $\pm$ .005	0.782 $\pm$ .004	10.936 $\pm$ .077	1.362 $\pm$ .062

requires 14.74s of average inference. While the MLD [2] reduces the average inference time to 0.217s by applying DDIM50 in latent space, we find this approach lacks the ability to edit and control motion by manipulating the model input.

To tackle this, we employ 1) efficient sampler, 2) embedded-text cache, 3) parallel CFG computation, and 4) low-precision inference to reduce iteration counts and network latency. As shown in Figure 1, our StableMoFusion significantly shortens the inference time and achieves higher performance within the original motion space.

However, it remains incontrovertible that StableMoFusion’s inference speed trails behind that of MLD, and fails to meet the industry’s real-time standard with an average inference time of 0.5s. Thus, our future work will focus on acceleration: the inference time of StableMoFusion is currently tied to the computation of the network, and we will further investigate how to scale down the model and how to reduce single-step latency in inference.

## 5.6 Ablation

### 5.6.1 Network Architecture.

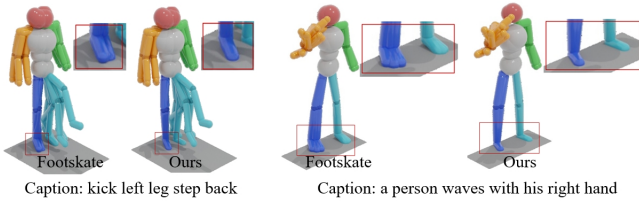


**Figure 5: Visualization comparison results before and after our footskate cleanup. The red bounding box shows details of skating feet.**

We assess the validity of the improvements over the baseline for all network architectures proposed in Section 4.1 with uniform training and inference processes.

Specifically, we evaluate the baseline and adjusted model (+cross-attention) of Conv1D UNet, DiT, and RetNet. As shown in Table 4, adding cross-attention notably boosts performance, highlighting its crucial role in enhancing the efficacy of conditional motion generation models.

Notably, *Conv1D UNet + cross-attention* achieves superior results on HumanML3D, and with slight adjustments to group normalization (+ *GroupNorm tweak*), also demonstrated robust performance on the KIT dataset. It proves that the GroupNorm tweak from sequence-wise normalization to feature-wise normalization on UNet is mainly useful for the datasets with dispersed length distributions, such as KIT-ML dataset.

**Table 4: Quantitative comparison of architectural improvements in UNet, DiT and RetNet.**

Dataset	Network	FID ↓	R Precision (top3) ↑
HumanML3D	Conv1D UNet baseline	0.245	0.780
	+ cross-attention	<b>0.074</b>	0.821
	+ GroupNorm Tweak	0.089	<b>0.840</b>
	DiT baseline	0.884	0.711
	+ cross-attention	0.113	0.787
	RetNet baseline	1.673	0.740
KIT-ML	+ cross-attention	0.147	0.853
	Conv1D UNet+ cross-attention + GroupNorm Tweak	0.658 <b>0.237</b>	0.756 <b>0.780</b>

### 5.6.2 Effective Inference.

By using the SDE variant of second-order DPM-Solver++ with Karras sigma, the inference process of diffusion-based motion generation is able to significantly reduce the minimum number of iterations required for generation from 1000 to 10 while enhancing the quality of generated motions, approximately 99% faster than the original inference process, as shown in Table 5.

The application of embedded text caching and parallel CFG further reduces the average inference time by about 0.3 seconds and 0.15 seconds, respectively. Our experiments also show that reducing the computational accuracy of the motion-denoising model by half, from FP32 to FP16, does not adversely affect the generation quality. This suggests that 32-bit precision is redundant for the motion generation task.

**Table 5: The progressive effect of each efficient and training-free trick of StableMoFusion in inference process.**

Method	FID ↓	R Precision (top3) ↑	AITs ↓	Inference Steps ↓
base (DDPM1000)	1.251	0.760	99.060	1000
+ Efficient Sampler	0.076	0.836	1.004(-99%)	10
+ Embedded-text Cache	0.076	0.836	0.690(-31%)	10
+ Parallel CFG	0.076	0.836	0.544(-21%)	10
+ FP16	0.076	0.837	0.499(-8%)	10

## 6 Conclusion

In this paper, we propose a robust and efficient diffusion-based motion generation framework, StableMoFusion, which uses Conv1DUNet as a motion-denoising network and employs two effective training strategies to enhance the network’s effectiveness, as well as four training-free tricks to achieve efficient inference. Extensive experimental results show that our StableMoFusion performs favorably against current state-of-the-art methods. Furthermore, we propose effective solutions for time-consuming inference and footskate problems, facilitating diffusion-based motion generation methods for practical applications in industry.

## References

- [1] Hanqun Cao, Cheng Tan, Zhangyang Gao, Yilun Xu, Guangyong Chen, Peng-Ann Heng, and Stan Z Li. A survey on generative diffusion model. *arXiv preprint arXiv:2209.02646*, 2022.
- [2] Xin Chen, Biao Jiang, Wen Liu, Zilong Huang, Bin Fu, Tao Chen, and Gang Yu. Executing your commands via motion diffusion in latent space. In *Proceedings of the IEEE/CVF Conference on Computer Vision and Pattern Recognition*, pages 18000–18010, 2023.
- [3] Rishabh Dabral, Muhammad Hamza Mughal, Vladislav Golyanik, and Christian Theobalt. Mofusion: A framework for denoising-diffusion-based motion synthesis. In *Proceedings of the IEEE/CVF Conference on Computer Vision and Pattern Recognition*, pages 9760–9770, 2023.
- [4] Wenxun Dai, Ling-Hao Chen, Jingbo Wang, Jinpeng Liu, Bo Dai, and Yansong Tang. Motionlcm: Real-time controllable motion generation via latent consistency model. *arXiv preprint arXiv:2404.19759*, 2024.
- [5] Prafulla Dhariwal and Alexander Nichol. Diffusion models beat gans on image synthesis. *Advances in neural information processing systems*, 34:8780–8794, 2021.
- [6] Chuan Guo, Shihao Zou, Xinxin Zuo, Sen Wang, Wei Ji, Xingyu Li, and Li Cheng. Generating diverse and natural 3d human motions from text. In *Proceedings of the IEEE/CVF Conference on Computer Vision and Pattern Recognition*, pages 5152–5161, 2022.
- [7] Xingjian Han, Benjamin Senderling, Stanley To, Deepak Kumar, Emily Whiting, and Jun Saito. Groundlink: A dataset unifying human body movement and ground reaction dynamics. In *ACM SIGGRAPH Asia 2023 Conference Proceedings*, pages 1–10, 2023.
- [8] Jonathan Ho, Ajay Jain, and Pieter Abbeel. Denoising diffusion probabilistic models. *Advances in neural information processing systems*, 33:6840–6851, 2020.
- [9] Biao Jiang, Xin Chen, Wen Liu, Jingyi Yu, Gang Yu, and Tao Chen. Motiongpt: Human motion as a foreign language. *Advances in Neural Information Processing Systems*, 36, 2024.
- [10] Yifeng Jiang, Jungdam Won, Yuting Ye, and C Karen Liu. Drop: Dynamics responses from human motion prior and projective dynamics. *SIGGRAPH Asia*, 2023.
- [11] Korrawe Karunratanakul, Konpat Preechakul, Supasorn Suwajanakorn, and Siyu Tang. Gmd: Controllable human motion synthesis via guided diffusion models. *arXiv preprint arXiv:2305.12577*, 2023.
- [12] Hanyang Kong, Kehong Gong, Dongze Lian, Michael Bi Mi, and Xinchao Wang. Priority-centric human motion generation in discrete latent space. In *Proceedings of the IEEE/CVF International Conference on Computer Vision*, pages 14806–14816, 2023.
- [13] Cheng Lu, Yuhao Zhou, Fan Bao, Jianfei Chen, Chongxuan Li, and Jun Zhu. Dpm-solver++: Fast solver for guided sampling of diffusion probabilistic models. *arXiv preprint arXiv:2211.01095*, 2022.
- [14] Lucas Mourot, Ludovic Hoyet, François Le Clerc, and Pierre Hellier. Underpressure: Deep learning for foot contact detection, ground reaction force estimation and footskate cleanup. *Computer Graphics Forum*, 41(8):195–206, December 2022.



- [15] William Peebles and Saining Xie. Scalable diffusion models with transformers. In *Proceedings of the IEEE/CVF International Conference on Computer Vision*, pages 4195–4205, 2023.
- [16] Matthias Plappert, Christian Mandery, and Tamim Asfour. The kit motion-language dataset. *arXiv preprint arXiv:1607.03827*, 2016.
- [17] Alec Radford, Jong Wook Kim, Chris Hallacy, Aditya Ramesh, Gabriel Goh, Sandhini Agarwal, Girish Sastry, Amanda Askell, Pamela Mishkin, Jack Clark, et al. Learning transferable visual models from natural language supervision. In *International conference on machine learning*, pages 8748–8763. PMLR, 2021.
- [18] Robin Rombach, Andreas Blattmann, Dominik Lorenz, Patrick Esser, and Björn Ommer. High-resolution image synthesis with latent diffusion models. In *Proceedings of the IEEE/CVF conference on computer vision and pattern recognition*, pages 10684–10695, 2022.
- [19] Yutao Sun, Li Dong, Shaohan Huang, Shuming Ma, Yuqing Xia, Jilong Xue, Jianyong Wang, and Furu Wei. Retentive network: A successor to transformer for large language models. *arXiv preprint arXiv:2307.08621*, 2023.
- [20] Guy Tevet, Sigal Raab, Brian Gordon, Yonatan Shafir, Daniel Cohen-Or, and Amit H Bermano. Human motion diffusion model. *arXiv preprint arXiv:2209.14916*, 2022.
- [21] Jonathan Tseng, Rodrigo Castellon, and C Karen Liu. Edge: Editable dance generation from music. *arXiv preprint arXiv:2211.10658*, 2022.
- [22] Yin Wang, Zhiying Leng, Frederick WB Li, Shun-Cheng Wu, and Xiaohui Liang. Fg-t2m: Fine-grained text-driven human motion generation via diffusion model. In *Proceedings of the IEEE/CVF International Conference on Computer Vision*, pages 22035–22044, 2023.
- [23] Yiming Xie, Varun Jampani, Lei Zhong, Deqing Sun, and Huaizu Jiang. Omnicon-trol: Control any joint at any time for human motion generation. In *The Twelfth International Conference on Learning Representations*, 2024.
- [24] Yilun Xu, Mingyang Deng, Xiang Cheng, Yonglong Tian, Ziming Liu, and Tommi Jaakkola. Restart sampling for improving generative processes. *arXiv preprint arXiv:2306.14878*, 2023.
- [25] Ye Yuan and Kris Kitani. Residual force control for agile human behavior imitation and extended motion synthesis. In *Advances in Neural Information Processing Systems*, 2020.
- [26] Ye Yuan, Jiaming Song, Umar Iqbal, Arash Vahdat, and Jan Kautz. Physdiff: Physics-guided human motion diffusion model. In *Proceedings of the IEEE/CVF International Conference on Computer Vision*, pages 16010–16021, 2023.
- [27] Jianrong Zhang, Yangsong Zhang, Xiaodong Cun, Shaoli Huang, Yong Zhang, Hongwei Zhao, Hongtao Lu, and Xi Shen. T2m-gpt: Generating human motion from textual descriptions with discrete representations. *arXiv preprint arXiv:2301.06052*, 2023.
- [28] Mingyuan Zhang, Zhongang Cai, Liang Pan, Fangzhou Hong, Xinying Guo, Lei Yang, and Ziwei Liu. Motiondiffuse: Text-driven human motion generation with diffusion model. *arXiv preprint arXiv:2208.15001*, 2022.
- [29] Mingyuan Zhang, Xinying Guo, Liang Pan, Zhongang Cai, Fangzhou Hong, Huirong Li, Lei Yang, and Ziwei Liu. Remodiffuse: Retrieval-augmented motion diffusion model. In *Proceedings of the IEEE/CVF International Conference on Computer Vision*, pages 364–373, 2023.